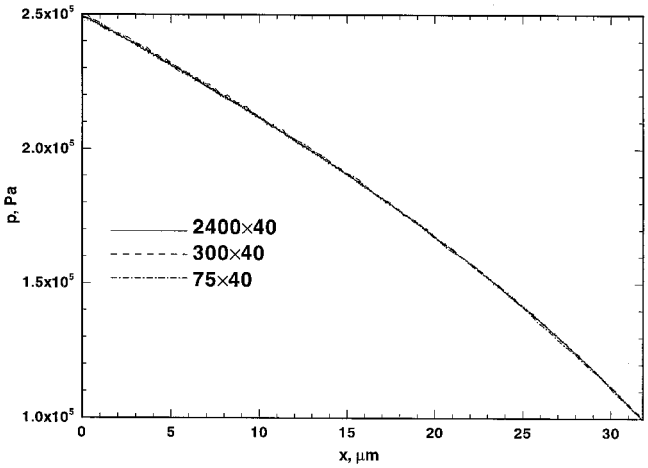

Fig. 2 Influence of grid resolution on centerline pressure distribution.

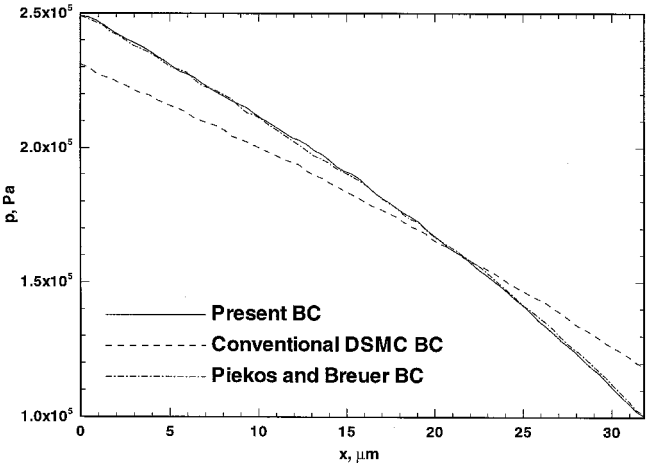

Fig. 3 Comparison of pressure distribution for new boundary conditions and standard DSMC boundary conditions.

This plot shows that results are virtually identical to those obtained with the boundary conditions proposed here. The agreement for other flow properties was found to be equally good.

In conclusion, we have proposed new DSMC boundary conditions suitable for use in low-speed MEMS applications. These conditions respect the proper directions of signal propagation for subsonic flows, and allow specification of inlet and exit pressures. Low-speed microchannel computations using these new conditions yield much better results than when traditional DSMC boundary conditions are used. However, the solutions are essentially the same as those obtained with the boundary conditions proposed by Piekos and Breuer.

Acknowledgments

This work was supported in part by NASA Cooperative Agreement NCC1-112 and a National Defense Science and Engineering Graduate Fellowship. Computer resources were provided by the Numerical Aerodynamic Simulation facilities at NASA Ames Research Center.

References

[1]Ho, C.-M., and Tai, Y.-C., "MEMS: Science and Technology," *Application of Microfabrication to Fluid Mechanics*, American Society of Mechanical Engineers, New York, 1994, pp. 39–49.

[2]Bird, G. A., *Molecular Gas Dynamics and the Direct Simulation of Gas Flows*, Clarendon, Oxford, England, UK, 1994.

[3]Piekos, E. S., and Breuer, K. S., "DSMC Modeling of Micromechanical Devices," AIAA Paper 95-2089, June 1995.

[4]Ikegawa, M., and Kobayashi, J., "Development of a Rarefied Flow Simulator Using the Direct-Simulation Monte Carlo Method," *JSME International Journal*, Series 2, Vol. 33, No. 3, 1990, pp. 463–467.

[5]Nance, R. P., Hash, D. B., and Hassan, H. A., "Role of Boundary Conditions in Monte Carlo Simulation of MEMS Devices," AIAA Paper 97-0375, Jan. 1997.

[6]Hwang, Y. S., Moon, B., Sharma, S., Ponnusamy, R., Das, R., and Saltz, J., "Runtime and Language Support for Compiling Adaptive Irregular Problems on Distributed Memory Machines," *Software Practice and Experience*, Vol. 25, No. 6, 1995, pp. 597–621.

[7]Nance, R. P., Wilmoth, R. G., Moon, B., Hassan, H. A., and Saltz, J., "Parallel Monte Carlo Simulation of Three-Dimensional Flow over a Flat Plate," *Journal of Thermophysics and Heat Transfer*, Vol. 9, No. 3, 1995, pp. 471–477.

[8]Whitfield, D. L., "Three-Dimensional Unsteady Euler Equation Solutions Using Flux Vector Splitting," Dec. 1983.

Re-Examination of Double Diffusive Natural Convection from Horizontal Surfaces in Porous Media

C. T. Li* and F. C. Lai†
University of Oklahoma,
Norman, Oklahoma 73019-0601

Introduction

COUPLED heat and mass transfer as a result of buoyancy in saturated porous media is frequently encountered in engineering applications. From a fundamental perspective, Nield[1] made the first attempt to study the stability of convective flow in horizontal layers with imposed vertical temperature and concentration gradients. This was followed by Khan and Zebib[2] in the study of flow stability in a vertical porous layer. Bejan and coworkers[3,4] conducted a series of investigations of these effects on natural convection in enclosures filled with porous medium. Other geometries considered in the previous studies include line sources,[5] vertical surfaces,[6] horizontal surfaces,[7,8] vertical cylinders,[9] and slender bodies of revolution.[10] Among these previous studies, it is noticed that similarity solutions for coupled heat and mass transfer by natural convection from horizontal surfaces have been reported for a special case of constant wall temperature and concentration.[7,8] It is speculated that these solutions might not be physically plausible because they did not satisfy the conditions imposed on the velocity, boundary-layer thickness, local heat flux, and total heat convected as suggested by Gebhart et al.[11] Thus, the purpose of the present study is to reinvestigate this fundamental problem to determine the limits within which a physically realistic similarity solution exists. Emphases have also been placed on a fundamental examination of these double-diffusion effects on the flow, temperature, and concentration fields. It is expected that the obtained results will not only complement the current literature but also provide useful information for engineering applications.

Presented as Paper 97-2516 at the AIAA 32nd Thermophysics Conference, Atlanta, GA, June 23–25, 1997; received Aug. 25, 1997; revision received Feb. 16, 1998; accepted for publication Feb. 16, 1998.

*Graduate Research Assistant, School of Aerospace and Mechanical Engineering.

†Associate Professor, School of Aerospace and Mechanical Engineering. Senior Member AIAA.

Analysis

Consider a horizontal surface embedded in a saturated porous medium. Having invoked the boundary-layer assumption and Boussinesq approximation, the governing equations in terms of the stream function are

$$\frac{\partial^2\psi}{\partial y^2} = \frac{Kg}{\nu}\left(\beta_T\frac{\partial T}{\partial x} + \beta_c\frac{\partial c}{\partial x}\right) \tag{1}$$

$$\frac{\partial\psi}{\partial y}\frac{\partial T}{\partial x} - \frac{\partial\psi}{\partial x}\frac{\partial T}{\partial y} = \alpha\frac{\partial^2 T}{\partial y^2} \tag{2}$$

$$\frac{\partial\psi}{\partial y}\frac{\partial c}{\partial x} - \frac{\partial\psi}{\partial x}\frac{\partial c}{\partial y} = D\frac{\partial^2 c}{\partial y^2} \tag{3}$$

In accordance with the linear Boussinesq approximation, the density is given by

$$\rho = \rho_\infty[1 - \beta_T(T - T_\infty) - \beta_c(c - c_\infty)] \tag{4}$$

where β_T and β_c are the coefficients for thermal and concentration expansion, respectively.

The corresponding boundary conditions are as follows.

At the surface ($y = 0$):

$$v = 0, \qquad T = T_w(x) = T_\infty + Ax^a, \qquad A > 0$$
$$c = c_w(x) = c_\infty + Bx^b, \qquad B > 0 \tag{5}$$

where the wall temperature and concentration are assumed to have a power-law variation.

At the infinity ($y \to \infty$):

$$u = 0, \qquad T = T_\infty, \qquad c = c_\infty \tag{6}$$

To solve the set of simultaneous equations defined in the preceding text, the following dimensionless variables are introduced:

$$\eta = Ra^{1/3}(y/x) \tag{7a}$$

$$\psi = \alpha Ra^{1/3} f(\eta) \tag{7b}$$

$$\theta = \frac{T - T_\infty}{T_w - T_\infty} \tag{7c}$$

$$C = \frac{c - c_\infty}{c_w - c_\infty} \tag{7d}$$

where $Ra = Kg\beta_T(T_w - T_\infty)x/\alpha\nu$ is the modified local Rayleigh number.

After transformation, the resulting equations are

$$f'' = \{(a\theta + bNC) + [(a - 2)/3]\eta(\theta' + NC')\} \tag{8}$$

$$\theta'' = af'\theta - [(a + 1)/3]f\theta' \tag{9}$$

$$C'' = Le\{bf'C - [(a + 1)/3]fC'\} \tag{10}$$

where parameter N [$=\beta_c(c_w - c_\infty)/\beta_T(T_w - T_\infty)$] measures the relative importance of mass and thermal diffusion in the buoyancy-driven flow. It is clear that N is zero for pure thermal buoyancy-driven flow; infinite for mass-driven flow; positive for aiding flow, i.e., enhancing thermal convection; and negative for opposing flow, i.e., suppressing thermal convection.

The corresponding boundary conditions are given by

$$\eta = 0, \qquad f = 0, \qquad \theta = 1, \qquad C = 1 \tag{11}$$

$$\eta \to \infty, \qquad f' \to 0, \qquad \theta \to 0, \qquad C \to 0 \tag{12}$$

To determine the ranges of a and b that permit physically realistic solutions, one needs to examine the variation of the streamwise velocity, boundary-layer thickness, local heat flux, local mass flux, total energy, and total species convected. To have physically realistic solutions, it is required that u, δ, Q, and M must be constant or increase with x, whereas q and m must be positive or at least zero.[11] These requirements lead to $1/2 \le a \le 2$ and $b \ge -(a + 1)/3$. It is clear that constant wall temperature ($a = 0$) and constant wall concentration ($b = 0$) are not in these ranges. Therefore, the solutions presented in the previous studies are not physically plausible.[7,8]

In the ranges specified a special case that permits similarity solutions is when the surface is under a constant heat flux ($a = 1/2$) and constant mass flux ($b = 1/2$) condition. For this case the governing equations are reduced to

$$f'' = \tfrac{1}{2}[(\eta\theta' - \theta) + N(\eta C' - C)] \tag{13}$$

$$\theta'' = \tfrac{1}{2}(f'\theta - f\theta') \tag{14}$$

$$C'' = (Le/2)[f'C - fC'] \tag{15}$$

It has been shown that similarity solutions exist for the case of pure thermal buoyancy-driven flow,[12] i.e., $N = 0$.

Results and Discussion

The transformed governing equations, along with the corresponding boundary conditions, are solved by the numerical integration using a fourth-order Runge–Kutta method and the shooting technique with a systematic guessing of $f'(0)$, $\theta'(0)$, and $C'(0)$. As an indication of proper formulation and accurate calculation, the results thus obtained have been compared with the data published earlier for the case of pure heat transfer-driven flows,[12] and they show excellent agreement. Calculations have been carried out for a wide range of the governing parameters, i.e., $-1 < N \le 10$ and $0.1 \le Le \le 100$, to verify the results obtained by scale analysis.[7]

It is important to note that for $N < 0$, solutions are not available for $N^2/Le \sim 1$. In this range the streamwise velocity becomes negative and the direction of buoyancy-induced flow is reversed, which contradicts the boundary-layer assumption and no solution is meaningful. For $Le > 1$, the contribution to the horizontal velocity by the mass buoyancy effect is less important and the flow reversal will occur at a smaller value of N. For $Le < 1$, the situation is reversed and the flow reversal will take place at a larger value of N.

The results of practical interest in many applications are the heat and mass transfer coefficients. The heat transfer coefficient in terms of the Nusselt number is given by

$$Nu = \frac{hx}{k} = -\frac{\partial T/\partial y\big|_{y=0}}{T_w - T_\infty} = -Ra^{1/3}\theta'(0) \tag{16}$$

whereas the mass transfer coefficient in terms of the Sherwood number is given by

$$Sh = \frac{mx}{D(c_w - c_\infty)} = -Ra^{1/3}C'(0) \tag{17}$$

The average heat and mass transfer coefficients can be readily derived from the preceding equations and they are given by

$$Nu_L = \frac{1}{L}\int_0^L Nu\,dx = -\frac{2}{3}Ra_L^{1/3}\theta'(0) \tag{18}$$

$$Sh_L = \frac{1}{L}\int_0^L Sh\,dx = -\frac{2}{3}Ra_L^{1/3}C'(0) \tag{19}$$

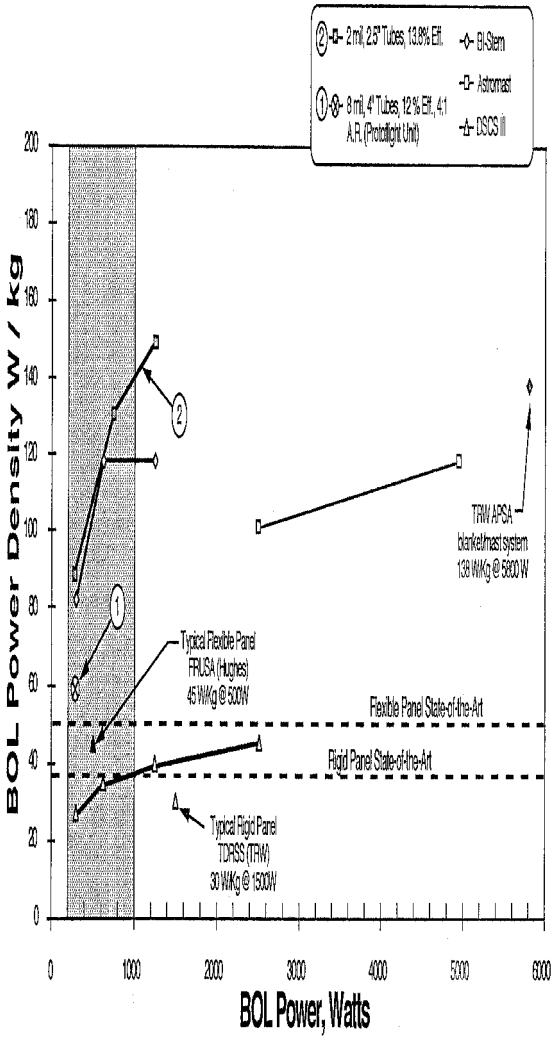

Fig. 1 Variation of streamwise velocity and heat and mass transfer coefficients with Lewis numbers.

The streamwise velocity and heat and mass transfer coefficients are plotted in Figs. 1 and 2 as a function of the Lewis number and buoyancy ratio, respectively. Following the scale analysis proposed by Bejan and Khair[3] and Jang and Chang,[7] the scale for these three variables can be obtained. For heat transfer-driven flows, i.e., $|N| << 1$, it is observed that the velocity and heat transfer coefficient approach an asymptotic value and become independent of Le when $Le \rightarrow 100$ (Fig. 1). For mass transfer coefficients it can be clearly observed that their dependence on the Lewis number has changed from Le (at small Lewis numbers) to $Le^{1/2}$ (at large Lewis numbers). For concentration driven flows, i.e., $|N| >> 1$, it is clearly shown that the velocity varies with $Le^{-1/3}$ and the mass transfer coefficient varies with $Le^{1/3}$ for a given buoyancy ratio, e.g., $N = 10$. The heat transfer coefficient, on the other hand, initially varies with $Le^{-1/6}$ at small Lewis numbers and changes to $Le^{-2/3}$ at large Lewis numbers before it approaches an asymptotic value.

The functional dependence of flow velocity and heat and mass transfer coefficients on the governing parameters Le and N discussed earlier can also be cross examined from Fig. 2. It is clear that the streamwise velocity is independent of Le and N for thermal buoyancy-driven flows ($|N| << 1$), whereas it varies with $|N|^{2/3}$ for mass transfer-driven flows. For the heat and mass transfer coefficients the present results also agree well with the scale analysis, i.e., they are independent of the buoyancy ratio for heat transfer-driven flows and vary with $|N|^{1/3}$ for mass transfer-driven flows.

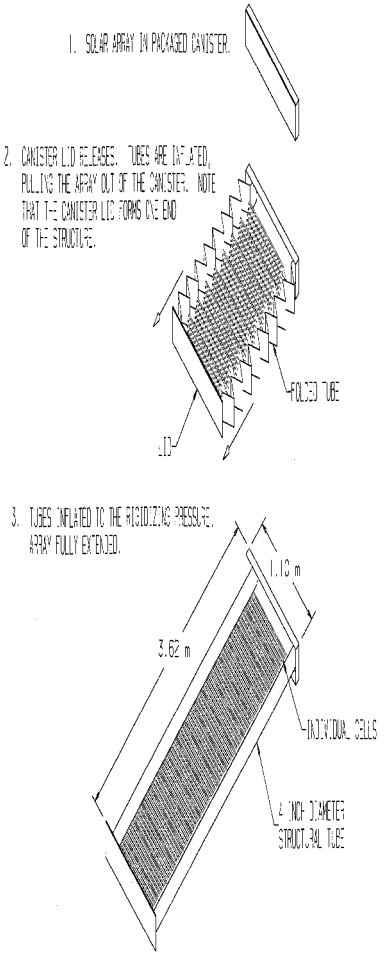

Fig. 2 Variation of streamwise velocity and heat and mass transfer coefficients with buoyancy ratios.

Conclusions

For coupled heat and mass transfer by natural convection from a horizontal surface in porous media, similarity solutions have been presented for a special case in which the surface heat flux and mass flux are maintained constant. The results thus obtained agree very well with the scale analysis. In addition, the present analysis shows that similarity solutions for a surface maintained at a constant temperature and concentration, as reported in the previous studies,[7,8] are not physically plausible. The present results are useful in many applications. For example these results are useful in the geophysical and geothermal applications where surface mass transfer on the bed (hot) rock is generated as a result of chemical reactions, and in the underground disposal of nuclear waste where the spreading of radioactive materials may result from the breakage of waste containers. Given the species properties, the present analysis can provide useful information in the estimate of life span of a viable geothermal reservoir or the traveling time required for radionuclides to reach the biosphere.

References

[1]Nield, D. A., "Onset of Thermohaline Convection in a Porous Medium," *Water Resources Research*, Vol. 4, No. 3, 1968, pp. 553–560.

[2]Khan, A. A., and Zebib, A., "Double Diffusive Instability in a Vertical Layer of a Porous Medium," *Journal of Heat Transfer*, Vol. 103, Feb. 1981, pp. 179–181.

[3]Bejan, A., and Khair, K. R., "Mass and Heat Transfer by Natural Convection in a Porous Medium," *International Journal of Heat and Mass Transfer*, Vol. 28, No. 5, 1985, pp. 909–918.

[4]Trevisan, O. V., and Bejan, A., "Natural Convection with Combined Heat and Mass Transfer Buoyancy Effects in a Porous Me-

dium," *International Journal of Heat and Mass Transfer*, Vol. 28, No. 8, 1985, pp. 1597–1611.

[5]Lai, F. C., "Coupled Heat and Mass Transfer by Natural Convection from a Horizontal Line Source in Saturated Porous Medium," *International Communications in Heat and Mass Transfer*, Vol. 17, No. 4, 1990, pp. 489–499.

[6]Lai, F. C., and F. A. Kulacki, "Coupled Heat and Mass Transfer by Natural Convection from Vertical Surfaces in Porous Media," *International Journal of Heat and Mass Transfer*, Vol. 34, No. 4/5, 1991, pp. 1189–1194.

[7]Jang, J.-Y., and Chang, W.-J., "The Flow and Vortex Instability of Horizontal Natural Convection in a Porous Medium Resulting from Combined Heat and Mass Buoyancy Effects," *International Journal of Heat and Mass Transfer*, Vol. 31, No. 4, 1988, pp. 769–777.

[8]Jang, J.-Y., and Chang, W.-J., "Buoyancy-Induced Inclined Boundary Layer Flow in a Porous Medium Resulting from Combined Heat and Mass Buoyancy Effects," *International Communications in Heat and Mass Transfer*, Vol. 15, No. 1, 1988, pp. 17–30.

[9]Yucel, A., "Natural Convection Heat and Mass Transfer Along a Vertical Cylinder in a Porous Medium," *International Journal of Heat and Mass Transfer*, Vol. 33, No. 10, 1990, pp. 2265–2274.

[10]Lai, F. C., Choi, C. Y., and Kulacki, F. A., "Coupled Heat and Mass Transfer by Natural Convection from Slender Bodies of Revolution in Porous Media," *International Communications in Heat and Mass Transfer*, Vol. 17, No. 5, 1990, pp. 609–620.

[11]Gebhart, B., Jaluria, Y., Mahajan, R. L., and Sammakia, B., *Buoyancy-Induced Flows and Transport*, Hemisphere, New York, 1988, pp. 54–64.

[12]Cheng, P., and Chang, I.-D., "Buoyancy Induced Flows in a Saturated Porous Medium Adjacent to Impermeable Horizontal Surfaces," *International Journal of Heat and Mass Transfer*, Vol. 19, No. 11, 1976, pp. 1267–1272.

Heat (Mass) Transfer in a Rotating Channel with Ribs of Various Sizes on Two Walls

C. W. Park,* S. C. Lau,† and R. T. Kukreja‡
Texas A&M University, College Station, Texas 77843

Introduction

NAPHTHALENE sublimation experiments have been conducted to study the effect of rib size on the heat (mass) transfer for radial outward flow in a rotating square channel with transverse ribs on the leading and trailing walls. The test channel modeled internal turbine blade cooling passages. Results were obtained for a Reynolds number Re of 5.5×10^3 and a rotation number Ro of 0.24, both of which were based on the hydraulic diameter of the test channel D.

Because the variation of the density of the naphthalene vapor–air mixture that passed through the test channel during an experiment was negligible, only the effects of the Coriolis force and the rib size, but not the buoyancy force, were examined. The results of this investigation may be used to improve numerical models for the design of cooling channels in turbine blades. The results should also help researchers and engineers better understand the effect of rib size on the heat (mass) transfer on the leading and trailing walls of a rotating channel.

Received Sept. 8, 1997; revision received Jan. 2, 1998; accepted for publication Jan. 13, 1998.

*Postdoctoral Associate, Mechanical Engineering.
†Associate Professor, Mechanical Engineering.
‡Research Engineer, Lynntech Inc., 7610 Eastmark Drive.

Test Apparatus and Procedure

The test apparatus, the instrumentation, and the test procedure for this study are the same as those used in Park et al.[1] Only a brief description is given in this Note.

The test section was an aluminum two-pass channel with a square cross section of 1.59 by 1.59 cm. The two straight segments were 0.11 m long. Naphthalene in shallow cavities covered the inner surfaces of the individual walls of the test section, so that the exposed surfaces of the test section walls were all mass transfer active during an experiment. In this investigation, attention was focused on the first straight pass only.

Ribs were cut from square balsa wood strips. The ribs were attached with epoxy transversely on two opposite walls of the first straight pass of the test channel. The exposed surfaces of the ribs were coated with naphthalene. The height of the ribs e ranged from 1/32 to 1/10 of the test channel hydraulic diameter. The rib arrays on the two walls were aligned. The rib spacing, or the pitch p, was equal to the test channel hydraulic diameter.

An entrance channel and an exit channel had the same square cross section as the test section and had lengths of 10 and 20 hydraulic diameters, respectively. The test section along with the entrance and exit channels rotated in a horizontal plane, with respect to a vertical axis, in a steel protective cage. The mean rotating radius of the test section was 30 times the test channel hydraulic diameter.

During a test run local elevation changes were measured at a grid of points on the naphthalene-coated surface of each of the two rib-roughened walls (537 points on each wall; 54 points between two ribs: 9 points along 6 lines that were parallel to the rib axes).

The local mass transfer coefficient is evaluated at each measurement point from the change of elevation at the point, the duration of the test run, and the difference between the naphthalene vapor density at the wall and the local bulk density of naphthalene in the airstream. The Sherwood number Sh is a dimensionless mass transfer coefficient based on the test channel hydraulic diameter and the diffusion coefficient for naphthalene vapor in air.[2] The Sherwood number is normalized by the corresponding Sherwood number for fully developed turbulent flow through a stationary smooth tube, $Sh_0 = 0.023Re^{0.8}Sc^{0.4}$. By applying the analogy between heat and mass transfer

$$Nu/Nu_0 = Sh/Sh_0 \tag{1}$$

where Nu is the Nusselt number and $Nu_0 = 0.023Re^{0.8}Pr^{0.4}$. Therefore, the normalized Sherwood number in this study may be considered as the ratio of the heat transfer coefficient for turbulent flow in a rotating square channel to that for the corresponding fully developed turbulent flow in a stationary tube with a hydraulic diameter equal to that of the square channel.

The maximum uncertainty of the Sherwood number is estimated to be 12.2%. The uncertainty of the Reynolds number is found to be 4.8%. The details of the data reduction procedure and the estimation of the experimental uncertainties are available in Park.[3]

In this Note attention is focused on the streamwise variations of the spanwise average Sherwood number ratio ($\overline{Sh}/Sh_0$) and the overall average Sherwood number ratios ($\overline{\overline{Sh}}/Sh_0$) on the leading and trailing walls over a typical pitch between two ribs. The detailed local mass transfer results and other average mass transfer results that are not included here are available in Park.[3]

Presentation and Discussion of Results

To examine the effect of varying the size of the trailing-wall ribs on the mass transfer on the leading and trailing walls, results have been obtained with leading-wall ribs of a fixed size (with either $D/e = p/e = 10$ or 16) and trailing-wall ribs